

CoRe: Joint Optimization with Contrastive Learning for Medical Image Registration

Eytan Kats¹, Christoph Grossbroehmer¹, Ziad Al-Haj Hemidi¹, Fenja Falta¹, Wiebke Heyer¹ and Mattias P. Heinrich^{1,*}

¹ Insitute of Medical Informatics, University of Luebeck, Luebeck, Germany

* Correspondence: mattias.heinrich@uni-luebeck.de

1. Introduction

Medical image registration is a fundamental problem in medical image analysis, aiming to establish dense anatomical and semantic correspondences between images. These images may be acquired at different time points, from different subjects, or using different imaging modalities. Accurate registration is a prerequisite for a wide range of downstream clinical and research tasks. It enables clinicians and researchers to track disease progression over time, evaluate the effectiveness of therapeutic interventions, quantify structural or functional changes, and analyze anatomical variability across patient populations.

The complexity of medical image registration arises primarily from two key factors: variability in image appearance and nonlinear anatomical deformations. Intensity variations commonly occur across scans due to differences in acquisition protocols, scanner hardware, or imaging modalities, making direct pixel-wise comparisons unreliable. Non-rigid deformations in anatomical structures are frequently observed in longitudinal scans of the same patient and in inter-subject comparisons within population studies. These deformations may also result from pathological changes or surgical interventions, adding further complexity to the registration process. To address these challenges, considerable research has focused on developing robust registration algorithms that can handle appearance variability while accurately modeling complex, spatially varying deformations.

Mutual information: The seminal work by Maes et al. [3] introduced mutual information (MI) as a similarity measure for the registration of multimodal medical images. Unlike traditional intensity-based metrics that rely on direct pixel value comparisons, MI quantifies the statistical dependence between images, enabling alignment based on their overall information content. Nevertheless, due to its statistical nature, MI is sensitive to noise and artifacts and is not suitable for complex nonlinear deformations.

Structural image representation: Traditional structural image representation methods [4–7] aim to extract spatially informative anatomical features that are more robust to intensity variations than raw pixel values. These approaches rely on hand-crafted descriptors designed to capture local structural patterns in a way that is less sensitive to differences in imaging protocols. While they do not explicitly model tissue deformations, such features are often more stable under small local changes. Registration algorithms then leverage these structural representations to estimate spatial transformations by comparing the similarity of the extracted features rather than relying directly on intensity values.

Supervised metric learning: Metric learning provides an alternative to traditional hand-crafted feature descriptors by leveraging deep neural networks to learn feature representations that minimize the distance between corresponding points in aligned image pairs [8,9]. This approach enables the extraction of discriminative features, tailored to capture complex anatomical variations and subtle tissue characteristics. However, supervised

Received:

Revised:

Accepted:

Published:

Copyright: © 2026 by the authors.

Submitted to *Sensors* for possible open access publication under the terms and conditions of the [Creative Commons Attribution \(CC BY\) license](#).

arXiv:2603.23694v1 [cs.CV] 24 Mar 2026

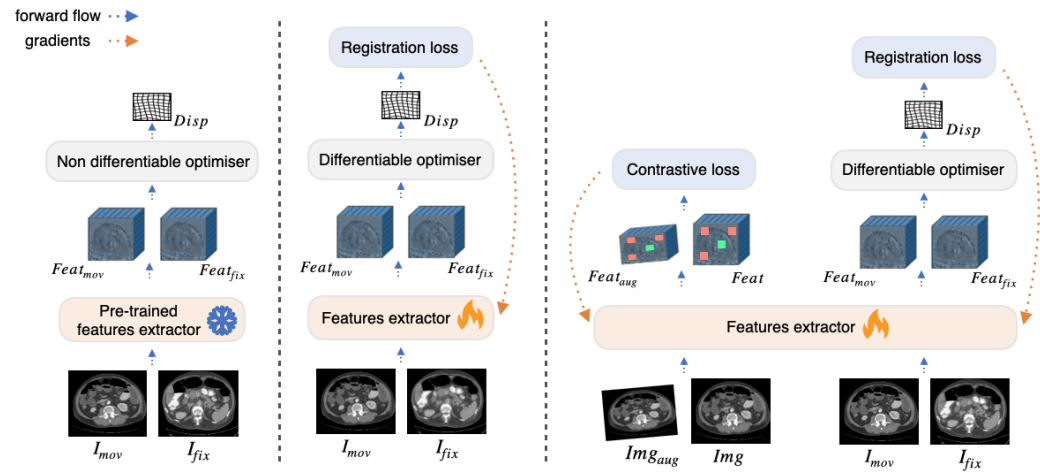


Figure 1. Comparison of hybrid registration methods. From left to right: (1) Feature extractor pretrained separately and used without further optimization during registration (SAMConvex [1]); (2) Feature extractor optimized exclusively with a registration loss during training (RegCyc [2]); (3) Proposed CoRe method, where the feature extractor is jointly optimized under both registration and contrastive loss objectives to enhance feature robustness and registration accuracy.

metric learning depends heavily on the availability of accurately aligned training data, which is often difficult and costly to obtain in medical imaging.

Self-supervised contrastive learning in medical imaging: Self-supervised contrastive learning has emerged as a powerful approach for representation learning in medical imaging, as it circumvents the need for explicit ground-truth annotations by enforcing consistency constraints on features extracted from augmented views of the same image [10–15]. This paradigm enables models to learn robust, semantically meaningful representations by maximizing agreement between different transformations of the same sample, thereby promoting generalization across diverse, unlabeled datasets. Within this framework, data augmentation plays a central role in shaping the learned feature space. Intensity-based augmentations and the addition of various noise types encourage the model to focus on anatomical structural features that remain robust despite fluctuations in image appearance and quality. Similarly, geometric transformations, such as rotations, scaling, and elastic deformations, are critical for fostering invariance to spatial changes, ensuring that the learned global embeddings are resilient to differences in orientation, scale, and shape. Recent research has further advanced this direction by introducing equivariance constraints into the training objective [16–18]. Unlike invariance, which aims to ignore certain transformations, equivariance ensures that specific transformations in the input space lead to predictable and structured changes in the embedding space. This property allows the model to distinguish between meaningful anatomical variability and non-informative deformations.

Contrastive learning in medical image registration: Recent studies have demonstrated the effectiveness of contrastive learning for generating dense feature representations that are well-suited to medical image registration tasks [1,16,19–21]. Existing methods in this space primarily differ in the stage at which feature extraction occurs relative to deformation estimation.

Some approaches perform feature extraction after the deformation field has been estimated. In this setting, features are computed from the fixed image and the deformed moving image, and the training objective is applied to corresponding feature representations. For instance, Mok et al. [20] pretrain a feature extractor using contrastive learning to enhance discriminability of anatomical structures across varying intensity profiles. During registration, the pretrained encoder is used to extract features from both fixed and

warped moving images, and a Mean Square Error (MSE) loss is applied between them. ContraReg [21] leverages a contrastive objective to train a registration model. It applies the contrastive loss to dense, multi-scale feature maps extracted from fixed and warped images using a pretrained autoencoder. In both approaches, the feature extractors are pretrained independently and kept fixed during the registration training phase.

Other methods extract features prior to deformation and use them as inputs to the registration model. CoMIR [16] employs supervised contrastive learning on aligned multimodal image pairs to project them into a shared latent space. These learned representations are then used to train a monomodal registration network in a separate stage. SAMConvex [1] and SAME [19] incorporate Self-supervised Anatomical embeddings (SAM) [14] to improve registration performance. SAMConvex combines SAM-based embeddings with decoupled convex optimization strategies [22,23], while SAME utilizes SAM to estimate affine transformations, produce coarse deformation fields, and integrates these estimates into the VoxelMorph framework [24].

Contributions: This paper introduces CoRe - Contrastive learning for medical image Registration¹, a novel approach that integrates self-supervised contrastive learning with deformable image registration through a unified, jointly optimized framework. By aligning feature learning with the downstream registration task, CoRe produces dense, semantically meaningful representations tailored for accurate deformation field estimation. CoRe follows the pre-deformation feature extraction paradigm, where features are extracted independently from fixed and moving images prior to deformation estimation. These features are then used by a differentiable optimization module to infer the deformation field.

Unlike existing approaches such as CoMIR [16], CoRe does not rely on known correspondences or paired multimodal training data. Instead, it leverages geometric augmentations of the same image to provide a self-supervised signal for contrastive learning. In contrast to SAMConvex [1], CoRe does not require a separate pretraining stage for the feature extractor. More importantly, it integrates knowledge of the registration task directly into the feature learning process via joint optimization, thereby aligning the learned representations with the requirements of the downstream registration module. As a result, the learned embeddings (1) capture semantic anatomical information that remains robust under tissue deformations and intensity variations, and (2) are inherently well-suited for driving the registration process through the optimization module.

The primary contributions of this work are as follows:

- We propose a novel joint optimization framework that integrates self-supervised contrastive learning directly into the registration pipeline, enhancing feature robustness to anatomical variability and improving overall registration performance.
- We demonstrate that simultaneous optimization of the contrastive and registration objectives leads to superior results compared to training with either objective alone, highlighting the synergy between representation learning and registration.
- We validate CoRe on abdominal and thoracic datasets in both intra-patient and inter-patient settings, where it achieves superior performance compared to competitive approaches.

2. Method

2.1. Problem definition

Let I_f, I_m denote the fixed and moving images, respectively. The training dataset consists of $|\Omega|$ image pairs $\Omega = \{I_f^s, I_m^s\}_{s=1}^{|\Omega|}$. The registration framework \mathcal{R} comprises a

¹ The code is available at <https://anonymous.4open.science/r/reg-ssl-D04E/>.

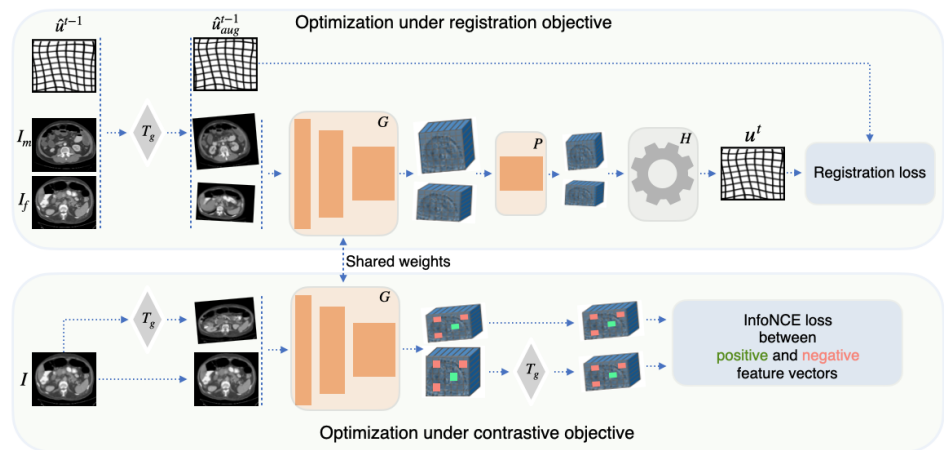


Figure 2. Overview of the proposed CoRe framework: The feature extractor is jointly optimized using registration and equivariance-based contrastive objectives, enabling robust and spatially coherent feature representations for precise displacement field estimation.

trainable feature extractor \mathcal{G} and a deterministic optimization module \mathcal{H} . Given I_f and I_m it predicts a displacement field $u = \mathcal{R}(I_f, I_m)$. Ideally, the intensity values $I_f(p)$ and $[Su \circ I_m](p)$ should correspond to the same anatomical location, where $[Su \circ I_m]$ represents I_m warped by the spatial transformation Su induced by u . The objective is to train \mathcal{G} to extract high-quality features, enabling \mathcal{H} to compute an optimal displacement field for accurate image alignment.

In this work, we incorporate equivariance constraints, formulated through a contrastive objective (Sec. 2.3), directly into the registration framework (Sec. 2.2). This integration ensures that the internal feature representations corresponding to identical anatomical locations remain robust to tissue deformations. Figure 2 presents an overview of the proposed joint optimization strategy, highlighting the simultaneous optimization of the feature extractor under both contrastive and registration objectives. Alg. 1 outlines the pseudo-code for the training procedure, detailing the steps involved in leveraging the synergistic interaction between these two objectives to enhance registration accuracy and robustness.

2.2. Registration framework

We use a hybrid registration pipeline comprising a convolutional feature extractor \mathcal{G} , a convolutional projection head \mathcal{P} , and a differentiable optimization module \mathcal{H} , which, given fixed and moving features, infers a displacement field that minimizes a combined objective of smoothness and feature dissimilarity. To achieve this, optimization module \mathcal{H} computes feature correlations over a discretized search window in a manner that remains differentiable with respect to the features [25]. The pipeline begins with \mathcal{G} extracting feature representations, $\mathcal{G}(I_f)$ and $\mathcal{G}(I_m)$, from the fixed and moving images, respectively. These representations are then passed through the projection head \mathcal{P} , and the resulting embeddings are processed by the optimizer \mathcal{H} , which predicts the displacement field u as follows:

$$u = \mathcal{R}(I_f, I_m) = \mathcal{H}(\mathcal{P}(\mathcal{G}(I_f)), \mathcal{P}(\mathcal{G}(I_m))). \quad (1)$$

We adopt the self-training scheme with pseudo-labels [2] as a strong baseline for deformable image registration. Training proceeds in M stages. At the beginning of each stage $t = 1, \dots, M$, the registration pipeline \mathcal{R} generates displacement fields u^{t-1} for all image pairs. These fields are refined through an iterative instance optimization,

which includes (1) enforcing forward-backward consistency on the displacement field, (2) applying a double warping procedure, and (3) performing iterative instance optimization. The refined displacement fields \hat{u}^{t-1} serve as pseudo-ground truth for supervising training of \mathcal{G} and \mathcal{P} during stage t . At the start of training, pseudo-labels \hat{u}^0 are generated using randomly initialized \mathcal{G} and \mathcal{P} . The training objective minimizes the mean squared error (MSE) loss between the displacement fields u^t predicted at training step of stage t and the pseudo-labels \hat{u}^{t-1} generated at the beginning of that stage:

$$\mathcal{L}_{\text{reg}} = \|u^t - \hat{u}^{t-1}\|^2. \quad (2)$$

To enhance the diversity of transformations during training, augmentation is applied to the pseudo displacement field (Figure 2). Specifically, the fixed and moving images, I_f and I_m , are each transformed using unique random affine augmentations T_g^f and T_g^m , respectively. The pseudo displacement field \hat{u} is then adjusted to account for these affine transformations, resulting in the augmented displacement field \hat{u}_{aug} .

2.3. Equivariance constraint

The quality of the displacement field u generated by the optimizer \mathcal{H} relies on the quality of the features extracted by the network \mathcal{G} . Ideally, the embeddings produced by \mathcal{G} for the same anatomical location in the moving image I_m and the fixed image I_f should be identical, regardless of geometric deformations between the images. Such consistency in feature embeddings provides \mathcal{H} with a robust initialization, allowing it to generate accurate displacement fields.

While the registration loss \mathcal{L}_{reg} (Sec. 2.2) naturally improves the features extracted by \mathcal{G} during training, we propose incorporating a contrastive objective to further refine feature quality. Specifically, to address the challenges posed by geometric deformations in tissue, we introduce an equivariance constraint on the image embeddings.

This constraint enforces consistency between embeddings derived from the same image I under geometric transformations. We apply an affine transformation $T_g \sim \mathcal{T}_g$, sampled from a predefined augmentation set \mathcal{T}_g , to the image I . The constraint ensures consistency between the transformed features of the original image, $G_A = T_g(\mathcal{G}(I))$, and the features of the transformed image, $G_B = \mathcal{G}(T_g(I))$. By enforcing this property, the model learns representations that are resilient to tissue deformations - an essential requirement for registration tasks, where features must remain consistent across anatomical distortions.

We implement the equivariance constraint using an InfoNCE loss [26] applied to feature vectors extracted from corresponding spatial locations in the feature maps G_A and G_B . Let f_A^j and f_B^j denote feature vectors sampled from the j th spatial location in G_A and G_B , where $j = 1, \dots, n$. Each feature vector f_A^j forms one positive pair with the corresponding vector f_B^j and $2 \cdot (n - 1)$ negative pairs with other feature vectors sampled from G_A and G_B . The contrastive loss is then defined as:

$$L_c = - \sum_j \log \frac{d(f_A^j, f_B^j)}{d(f_A^j, f_B^j) + \sum_{l \neq j} \sum_{k \in A, B} d(f_A^j, f_k^l)}, \quad (3)$$

where $d(f_A^j, f_B^j) = \exp(\langle f_A^j, f_B^j \rangle / \tau)$, $\langle \cdot, \cdot \rangle$ denotes the inner product, and τ is a temperature scaling factor that controls the sharpness of the similarity distribution. In our experiments, we set $\tau = 0.1$.

2.4. Joint optimization

By jointly minimizing the registration loss (Sec.2.2) and the contrastive loss (Sec.2.3), the proposed framework ensures that the feature representations extracted by the network

```
for I_f, I_m, disp_gt in data_loader:

    # apply random affine transform
    I_f_aug, I_m_aug, disp_aug, T_f, T_m = aug_affine(I_f, I_m,
                                                    disp_gt)

    # extract features from not augmented images
    feat_f = feature_extractor(I_f)
    feat_m = feature_extractor(I_m)

    # extract features from augmented images
    feat_f_aug_A = feature_extractor(I_f_aug)
    feat_m_aug_A = feature_extractor(I_m_aug)

    # extract projections from augmented features
    proj_f = projector(feat_f_aug_A)
    proj_m = projector(feat_m_aug_A)

    # generate displacement field
    disp = get_disp(proj_f, proj_m)

    # calculate registration loss
    L_reg = MSE(disp_aug, disp_gt)

    # transform features of not augmented images
    feat_f_aug_B = transform_feat(T_aff_f, feat_f)
    feat_m_aug_B = transform_feat(T_aff_m, feat_m)

    # calculate contrastive loss
    L_cl_f = InfoNCE(feat_f_aug_A, feat_f_aug_B)
    L_cl_m = InfoNCE(feat_m_aug_A, feat_m_aug_B)

    # calculate total loss
    L_total = L_reg + alpha * (L_cl_f + L_cl_m)

    # update weights
    loss.backward()
    optimizer.update([encoder, projector])
```

Listing 1: Pseudocode of the training procedure in PyTorch-like style.

Table 1. Quantitative results for AbdomenCT and RadChestCT registration tasks. The proposed CoRe method outperforms all comparison methods in terms of Dice, with statistical significance confirmed by a Wilcoxon signed-rank test ($p < 0.0001$), underscoring the advantages of the joint optimization strategy. The smoothness of the predicted displacement fields (SDlogJ) remains low and comparable to other methods.

Method	AbdomenCT			RadChestCT		
	DSC \uparrow	SDLogJ \downarrow	T_{inf} \downarrow	DSC \uparrow	SDLogJ \downarrow	T_{inf} \downarrow
Initial	25.9 \pm 7.1	–	–	34.1 \pm 14.5	–	–
DEEDs	46.5 \pm 8.1	0.058	45.2 s	88.5 \pm 6.9	0.049	45.0 s
NiftyReg	34.9 \pm 9.3	0.034	123.5 s	84.4 \pm 7.4	0.021	85.5 s
VoxelMorph	35.4 \pm 8.9	0.134	0.2 s	55.6 \pm 10.3	0.101	0.3 s
LapIRN	42.4 \pm 8.2	0.089	0.7 s	83.4 \pm 7.6	0.075	0.8 s
SAMConvex	49.2 \pm 7.8	0.096	5.1 s	88.1 \pm 7.1	0.079	6.4 s
RegCyc	51.1 \pm 7.3	0.146	1.2 s	87.3 \pm 6.9	0.106	1.9 s
CoRe (ours)	52.1 \pm 7.5	0.148	1.2 s	89.4 \pm 6.6	0.109	1.9 s

\mathcal{G} are robust to geometric transformations while remaining well-suited to the optimization procedure defined by the optimizer \mathcal{H} . The registration loss drives the alignment of fixed and moving images, encouraging the feature extractor to generate embeddings that are specifically tailored for consumption by the optimizer. Concurrently, the contrastive loss provides valuable guidance to the optimization process by imposing equivariance to geometric distortions, fostering the consistency of feature embeddings for same anatomical locations in registered images. The joint optimization process integrates the strengths of both losses, improving the robustness and accuracy of the registration framework. The combined loss function is defined as:

$$L = L_{reg} + \alpha \cdot L_c, \quad (4)$$

where α is a weighting coefficient that balances the contributions of the contrastive loss and the registration objective.

3. Experiments and results

3.1. Datasets and evaluation metrics

We evaluate the performance of the proposed method on the challenging inter-patient abdominal CT registration dataset [27]. This dataset comprises 30 3D abdominal CT scans from different patients, with 13 manually labeled anatomical structures: spleen, right kidney, left kidney, gall bladder, esophagus, liver, stomach, aorta, inferior vena cava, portal and splenic vein, pancreas, left adrenal gland, and right adrenal gland. All images are resampled to a uniform voxel resolution of 2 mm and standardized to spatial dimensions of $192 \times 160 \times 256$ voxels. The training-test split of this dataset defined in Learn2Reg challenge [28] widely adapted in the medical image registration community which facilitates direct comparison with prior works. Specifically, the training set includes 20 scans (190 image pairs), while the test set consists of 10 scans (45 image pairs).

To evaluate performance in the intra-patient setting, we utilize the RAD-ChestCT dataset [29]. In this dataset, we identified 371 longitudinal scan pairs. We split the data to 300 pairs designated for training and 71 pairs for testing. The CT images are resampled to a consistent voxel resolution of 1.5 mm and spatial dimensions of $256 \times 256 \times 224$ voxels. Since the RAD-ChestCT dataset does not include manual segmentation labels, we employ the TotalSegmentator tool [30] to segment the CT scans. Using the resulting segmentations,

we calculate registration accuracy across 22 anatomical structures: 5 lung lobes, vertebrae from T1 to T12, heart myocardium, left and right heart ventricles and atriums.

To assess accuracy of the registration, we compute the average Dice similarity coefficient (*DSC*) using available segmented structures. The plausibility of the deformation fields is evaluated using the standard deviation of the logarithm of the Jacobian determinant (*SDlogJ*). Additionally, we report inference run-time (T_{inf}) across methods.

3.2. Implementation details

The feature extractor \mathcal{G} is composed of four convolutional blocks, where each block includes a 3D convolutional layer with a kernel size of $3 \times 3 \times 3$ followed by a batch normalization layer and a ReLU activation function. The projection head \mathcal{P} consists of a single convolutional block with 128 output channels, a kernel size of $3 \times 3 \times 3$, and a stride of 2, followed by a final convolutional layer with a kernel size of $1 \times 1 \times 1$, which projects the feature maps to 16 channels. The framework is trained for $M = 8$ stages, with each stage consisting of 1000 iterations and a batch size of 2. Optimization is performed using the Adam optimizer, and the learning rate follows a cosine annealing warm restart schedule, decaying from $1 \cdot 10^{-3}$ to $1 \cdot 10^{-5}$. The contrastive loss is applied to the output of the final block's convolutional layer, with 1,000 feature vectors sampled per image pair.

3.3. Registration results

We compare our method with two conventional registration approaches (NiftyReg [31] and DEEDs [32]), two learning-based methods (VoxelMorph [24] and LapIRN [33]), and two hybrid approaches (RegCyc [2] and SAMConvex [1]) (Table 1). NiftyReg utilizes a four-level multi-resolution strategy, adaptive gradient descent optimization, and mutual information (MI) as the similarity measure. DEEDs aligns images using edge-based similarity and employs a B-spline transformation model with diffusion regularization. VoxelMorph and LapIRN predict dense displacement fields directly from input image pairs via a CNN, with LapIRN refining displacement fields across multiple resolutions. RegCyc and SAMConvex are hybrid approaches that leverage CNNs for feature extraction from image pairs and classical optimization techniques for displacement field estimation. SAMConvex uses a pretrained SAM model [14] for feature extraction, while RegCyc optimizes the feature extractor with a differentiable optimizer and registration loss (Figure 1).

Learnable approaches are computationally efficient, however, they often underperform compared to traditional and hybrid methods. DEEDs achieves strong results on the RadChestCT dataset, ranking as the second-best method. This performance is expected due to its focus on optimizing edge similarity, which is highly effective for intra-patient thoracic datasets where edges in image pairs align closely. However, on the AbdomenCT dataset, where deformations between image pairs are more complex, DEEDs demonstrates lower accuracy compared to hybrid methods. Hybrid approaches combine deep learning's ability to extract robust features with the precision and reliability of classical optimization techniques for displacement field estimation. This synergy enables hybrid methods to achieve state-of-the-art performance on the challenging inter-patient AbdomenCT dataset while maintaining competitive results on RadChestCT. Our proposed CoRe method achieves the best performance on both datasets, delivering the highest Dice scores (*DSC*) while preserving smoothness in the predicted displacement fields (*SDLogJ*), comparable to competitive methods. These results underscore the effectiveness of our approach, which incorporates an equivariance-based contrastive objective directly into the registration framework, enabling performance improvement for image registration tasks. Figure 3 presents qualitative registration results of the proposed method on the AbdomenCT and RadChestCT datasets.

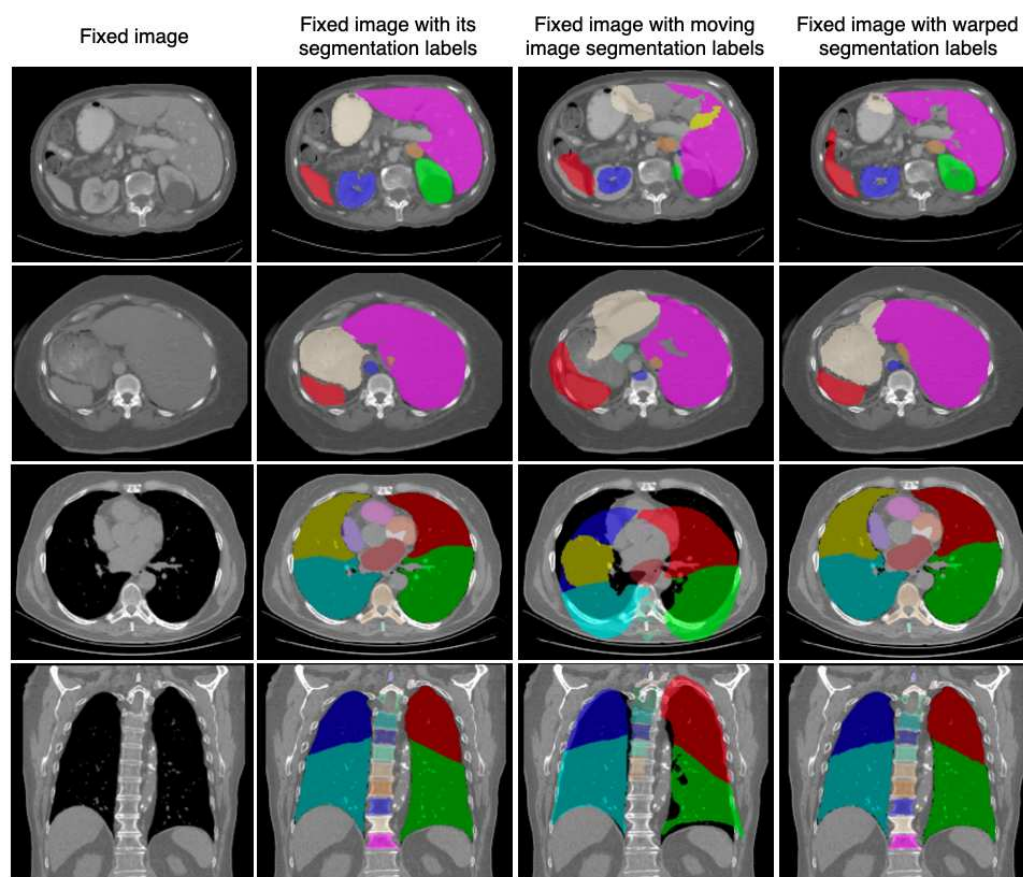


Figure 3. Qualitative results of the proposed CoRe method. From left to right: fixed image, fixed image with its segmentation overlay, fixed image with the overlay of the moving image segmentation, and fixed image with the overlay of the warped segmentation. The top two rows show examples from the AbdomenCT dataset in the axial plane, while the bottom two rows present examples from the RadChestCT dataset in axial and coronal planes.

3.4. Ablations study

To assess the effectiveness of the proposed method, we trained the feature extractor \mathcal{G} using regularization loss and contrastive loss independently and compared the results with the proposed joint optimization approach (Table 2). For the contrastive loss, we initially pretrained \mathcal{G} using only contrastive objective and subsequently trained the registration framework with \mathcal{G} frozen using only registration objective. The joint optimization approach demonstrates superior performance, underscoring the synergistic benefits of combining these objectives. This strategy facilitates the extraction of more discriminative and spatially coherent features, enhancing registration accuracy across datasets.

Along with the equivariance constraint described in Sec. 2.3, self-supervised contrastive learning methods commonly employ non-linear intensity augmentations during pretraining to encourage feature invariance to variations in appearance while preserving spatial encoding. To evaluate the impact of these augmentations on the registration task, we trained our framework with geometric equivariance and appearance invariance constraints both independently and jointly. Interestingly, the results reveal that within the proposed framework, non-linear intensity augmentations do not provide additional benefits over training solely with the geometric equivariance constraint. For the AbdomenCT dataset, training with intensity augmentations for contrastive loss even results in inferior performance compared to using the registration objective alone. We hypothesize that this is due to the mono-modal nature of the CT datasets used in our evaluation. The standardized

Table 2. Comparison of training the feature extractor with registration and contrastive objectives separately and jointly. The proposed joint optimization strategy achieves the best performance.

\mathcal{L}_{reg}	\mathcal{L}_{cl}	AbdomenCT		RadChestCT	
		DSC \uparrow	SDLogJ \downarrow	DSC \uparrow	SDLogJ \downarrow
✓		51.1 \pm 7.3	0.146	87.3 \pm 6.9	0.106
	✓	50.3 \pm 7.5	0.151	86.7 \pm 7.1	0.117
✓	✓	52.1 \pm 7.5	0.148	89.4 \pm 6.6	0.109

Table 3. Comparison of the effect of intensity invariance and geometric equivariance constraints, applied separately and jointly. Training with the equivariance constraint achieves the best performance, highlighting the importance of feature robustness to non-linear tissue deformations.

T_i	T_g	AbdomenCT		RadChestCT	
		DSC \uparrow	SDLogJ \downarrow	DSC \uparrow	SDLogJ \downarrow
		51.1 \pm 7.3	0.146	87.3 \pm 6.9	0.106
✓		49.4 \pm 8.1	0.139	87.5 \pm 7.0	0.115
	✓	52.1 \pm 7.5	0.148	89.4 \pm 6.6	0.109
✓	✓	50.2 \pm 7.6	0.138	89.3 \pm 6.5	0.102

intensity values in the CT datasets may limit the effectiveness of intensity augmentations, as they do not enhance the discriminative capacity of the learned features. Future work may explore the utility of intensity augmentations in multi-modal settings or datasets with greater intensity variability, where these augmentations could play a more significant role in improving registration performance.

4. Discussion

We introduced CoRe, a hybrid image registration framework that effectively integrates contrastive learning into the registration pipeline. We demonstrated that jointly optimizing the feature extractor under both contrastive and registration objectives facilitates the learning of spatially coherent and discriminative features, tailored to the requirements of classical optimization procedures. Our findings emphasize the important role of equivariant geometric constraints, implemented through contrastive loss, in enabling the extraction of robust features. These features are particularly effective in handling tissue deformations, improving performance of the registration task. Quantitative results on the AbdomenCT and RadChestCT datasets confirm that CoRe consistently outperforms state-of-the-art conventional, learning-based, and hybrid registration methods, achieving superior Dice scores while maintaining competitive smoothness of displacement fields.

These results highlight the potential of directly integrating contrastive learning into the registration framework to improve medical image registration performance. By leveraging the synergies of joint optimization, CoRe offers a robust and precise framework for efficient image alignment, presenting a promising direction for future exploration in this domain.

Author Contributions: Conceptualization, E.K. and M.H.; methodology, E.K.; software, E.K.; validation, E.K., C.G., Z.H., F.F. and W.H.; formal analysis, E.K.; investigation, E.K.; resources, M.H.; data curation, E.K.; writing—original draft preparation, E.K.; writing—review and editing, E.K. and M.H.; visualization, E.K.; supervision, M.H.; project administration, M.H.; funding acquisition, M.H. All authors have read and agreed to the published version of the manuscript.

Funding: This research was funded by German Research Foundation: DFG, HE 7364/10-1, project number 500498869.

Data Availability Statement: The datasets analyzed in this study are publicly accessible through third-party repositories. The inter-patient abdominal CT registration dataset [27] is available via Zenodo at <https://doi.org/10.5281/zenodo.3715652>. The RAD-ChestCT dataset is available via Zenodo at <https://doi.org/10.5281/zenodo.6406114>.

Conflicts of Interest: The authors declare no conflicts of interest. The funders had no role in the design of the study; in the collection, analyses, or interpretation of data; in the writing of the manuscript; or in the decision to publish the results.

References

1. Li, Z.; Tian, L.; Mok, T.C.; Bai, X.; Wang, P.; Ge, J.; Zhou, J.; Lu, L.; Ye, X.; Yan, K.; et al. Samconvex: Fast discrete optimization for ct registration using self-supervised anatomical embedding and correlation pyramid. In Proceedings of the International Conference on Medical Image Computing and Computer-Assisted Intervention. Springer, 2023, pp. 559–569.
2. Bigalke, A.; Hansen, L.; Mok, T.C.; Heinrich, M.P. Unsupervised 3d registration through optimization-guided cyclical self-training. In Proceedings of the International Conference on Medical Image Computing and Computer-Assisted Intervention. Springer, 2023, pp. 677–687.
3. Maes, F.; Collignon, A.; Vandermeulen, D.; Marchal, G.; Suetens, P. Multimodality image registration by maximization of mutual information. *IEEE Transactions on Medical Imaging* **1997**, *16*, 187–198.
4. Borvornvitchotikarn, T.; Kurutach, W. mirid: Multi-modal image registration using modality-independent and rotation-invariant descriptor. *Symmetry* **2020**, *12*, 2078.
5. Heinrich, M.P.; Jenkinson, M.; Bhushan, M.; Matin, T.; Gleeson, F.V.; Brady, M.; Schnabel, J.A. MIND: Modality independent neighbourhood descriptor for multi-modal deformable registration. *Medical Image Analysis* **2012**, *16*, 1423–1435.
6. Jiang, D.; Shi, Y.; Yao, D.; Wang, M.; Song, Z. miLBP: a robust and fast modality-independent 3D LBP for multimodal deformable registration. *International journal of computer assisted radiology and surgery* **2016**, *11*, 997–1005.
7. Jaouen, V.; Conze, P.H.; Dardenne, G.; Bert, J.; Visvikis, D. Regularized directional representations for medical image registration. *arXiv preprint arXiv:2111.15509* **2021**.
8. Simonovsky, M.; Gutiérrez-Becker, B.; Mateus, D.; Navab, N.; Komodakis, N. A deep metric for multimodal registration. In Proceedings of the Medical Image Computing and Computer-Assisted Intervention-MICCAI 2016: 19th International Conference, Athens, Greece, October 17–21, 2016, Proceedings, Part III 19. Springer, 2016, pp. 10–18.
9. Blendowski, M.; Heinrich, M.P. Combining MRF-based deformable registration and deep binary 3D-CNN descriptors for large lung motion estimation in COPD patients. *International journal of computer assisted radiology and surgery* **2019**, *14*, 43–52.
10. Wang, X.; Zhang, R.; Shen, C.; Kong, T.; Li, L. Dense contrastive learning for self-supervised visual pre-training. In Proceedings of the Proceedings of the IEEE/CVF conference on computer vision and pattern recognition, 2021, pp. 3024–3033.
11. Chaitanya, K.; Erdil, E.; Karani, N.; Konukoglu, E. Contrastive learning of global and local features for medical image segmentation with limited annotations. *Advances in neural information processing systems* **2020**, *33*, 12546–12558.
12. Goncharov, M.; Soboleva, V.; Kurmukov, A.; Pisov, M.; Belyaev, M. vox2vec: A framework for self-supervised contrastive learning of voxel-level representations in medical images. In Proceedings of the International Conference on Medical Image Computing and Computer-Assisted Intervention. Springer, 2023, pp. 605–614.
13. Kats, E.; Hirsch, J.G.; Heinrich, M.P. Self-supervised Learning of Dense Hierarchical Representations for Medical Image Segmentation. *arXiv preprint arXiv:2401.06473* **2024**.
14. Yan, K.; Cai, J.; Jin, D.; Miao, S.; Guo, D.; Harrison, A.P.; Tang, Y.; Xiao, J.; Lu, J.; Lu, L. SAM: Self-supervised learning of pixel-wise anatomical embeddings in radiological images. *IEEE Transactions on Medical Imaging* **2022**, *41*, 2658–2669.
15. Bai, X.; Bai, F.; Huo, X.; Ge, J.; Lu, J.; Ye, X.; Yan, K.; Xia, Y. SAMv2: A Unified Framework for Learning Appearance, Semantic and Cross-Modality Anatomical Embeddings. *arXiv preprint arXiv:2311.15111* **2023**.
16. Pielawski, N.; Wetzler, E.; Öfverstedt, J.; Lu, J.; Wählby, C.; Lindblad, J.; Sladoje, N. CoMIR: Contrastive multimodal image representation for registration. *Advances in neural information processing systems* **2020**, *33*, 18433–18444.
17. Seince, M.; Folgoc, L.L.; de Souza, L.A.F.; Angelini, E. Dense Self-Supervised Learning for Medical Image Segmentation. *arXiv preprint arXiv:2407.20395* **2024**.
18. Santhirasekaram, A.; Winkler, M.; Rockall, A.; Glocker, B. A geometric approach to robust medical image segmentation. *Medical Image Analysis* **2024**, *97*, 103260.
19. Liu, F.; Yan, K.; Harrison, A.P.; Guo, D.; Lu, L.; Yuille, A.L.; Huang, L.; Xie, G.; Xiao, J.; Ye, X.; et al. SAME: Deformable image registration based on self-supervised anatomical embeddings. In Proceedings of the Medical Image Computing and Computer Assisted Intervention–MICCAI 2021: 24th International Conference, Strasbourg, France, September 27–October 1, 2021, Proceedings, Part IV 24. Springer, 2021, pp. 87–97.

20. Mok, T.C.; Li, Z.; Bai, Y.; Zhang, J.; Liu, W.; Zhou, Y.J.; Yan, K.; Jin, D.; Shi, Y.; Yin, X.; et al. Modality-Agnostic Structural Image Representation Learning for Deformable Multi-Modality Medical Image Registration. In Proceedings of the IEEE/CVF Conference on Computer Vision and Pattern Recognition, 2024, pp. 11215–11225.
21. Dey, N.; Schlemper, J.; Salehi, S.S.M.; Zhou, B.; Gerig, G.; Sofka, M. Contrareg: Contrastive learning of multi-modality unsupervised deformable image registration. In Proceedings of the International Conference on Medical Image Computing and Computer-Assisted Intervention. Springer, 2022, pp. 66–77.
22. Siebert, H.; Hansen, L.; Heinrich, M.P. Fast 3D registration with accurate optimisation and little learning for Learn2Reg 2021. In Proceedings of the International Conference on Medical Image Computing and Computer-Assisted Intervention. Springer, 2021, pp. 174–179.
23. Heinrich, M.P.; Papież, B.W.; Schnabel, J.A.; Handels, H. Non-parametric discrete registration with convex optimisation. In Proceedings of the International Workshop on Biomedical Image Registration. Springer, 2014, pp. 51–61.
24. Balakrishnan, G.; Zhao, A.; Sabuncu, M.R.; Guttag, J.; Dalca, A.V. Voxelmorph: a learning framework for deformable medical image registration. *IEEE Transactions on Medical Imaging* **2019**, *38*, 1788–1800.
25. Siebert, H.; Heinrich, M.P. Learn to fuse input features for large-deformation registration with differentiable convex-discrete optimisation. In Proceedings of the International Workshop on Biomedical Image Registration. Springer, 2022, pp. 119–123.
26. Chen, T.; Kornblith, S.; Norouzi, M.; Hinton, G. A simple framework for contrastive learning of visual representations. In Proceedings of the International conference on machine learning. PMLR, 2020, pp. 1597–1607.
27. Xu, Z.; Lee, C.P.; Heinrich, M.P.; Modat, M.; Rueckert, D.; Ourselin, S.; Abramson, R.G.; Landman, B.A. Evaluation of six registration methods for the human abdomen on clinically acquired CT. *IEEE Transactions on Biomedical Engineering* **2016**, *63*, 1563–1572.
28. Hering, A.; Hansen, L.; Mok, T.C.; Chung, A.C.; Siebert, H.; Häger, S.; Lange, A.; Kuckertz, S.; Heldmann, S.; Shao, W.; et al. Learn2Reg: comprehensive multi-task medical image registration challenge, dataset and evaluation in the era of deep learning. *IEEE Transactions on Medical Imaging* **2022**, *42*, 697–712.
29. Draelos, R.L.; Dov, D.; Mazurowski, M.A.; Lo, J.Y.; Henao, R.; Rubin, G.D.; Carin, L. Machine-learning-based multiple abnormality prediction with large-scale chest computed tomography volumes. *Medical image analysis* **2021**, *67*, 101857.
30. Wasserthal, J.; Breit, H.C.; Meyer, M.T.; Pradella, M.; Hinck, D.; Sauter, A.W.; Heye, T.; Boll, D.T.; Cyriac, J.; Yang, S.; et al. TotalSegmentator: robust segmentation of 104 anatomic structures in CT images. *Radiology: Artificial Intelligence* **2023**, *5*, e230024.
31. Modat, M.; Ridgway, G.R.; Taylor, Z.A.; Lehmann, M.; Barnes, J.; Hawkes, D.J.; Fox, N.C.; Ourselin, S. Fast free-form deformation using graphics processing units. *Computer methods and programs in biomedicine* **2010**, *98*, 278–284.
32. Heinrich, M.P.; Jenkinson, M.; Brady, M.; Schnabel, J.A. MRF-based deformable registration and ventilation estimation of lung CT. *IEEE transactions on medical imaging* **2013**, *32*, 1239–1248.
33. Mok, T.C.; Chung, A.C. Large deformation diffeomorphic image registration with laplacian pyramid networks. In Proceedings of the International Conference on Medical Image Computing and Computer-Assisted Intervention. Springer, 2020, pp. 211–221.

Disclaimer/Publisher’s Note: The statements, opinions and data contained in all publications are solely those of the individual author(s) and contributor(s) and not of MDPI and/or the editor(s). MDPI and/or the editor(s) disclaim responsibility for any injury to people or property resulting from any ideas, methods, instructions or products referred to in the content.